English Translation by Cory Pye. This translation is provided as-is for ease of understanding by English readers. Permission granted by Dr. Xia Yang, Managing Editor of *Acta Chimica Sinica*, Feb 7, 2022.

Translation of *Acta Chimica Sinica*, **71**, 1307-1312 (2013) DOI: 10.6023/A13040368

Density functional and molecular dynamics studies on the hydrated structure of Pb(II)

Wang Juan[a,b] Xia Shuwei[*1,a] Yu Liangmin[a]

([a] Key Laboratory of Ocean Chemistry Theory and Engineering Technology, Ministry of Education, Ocean University of China, Qingdao 266100)

([b] School of Chemistry and Pharmacy, Qingdao Agricultural University, Qingdao 266109)

Abstract The hydration structure of Pb(II) in aqueous solution lacks experimental data, and the bonding mechanism is still unclear. The low-energy conformation of hydrated species $Pb(H_2O)_{1\text{-}9}^{2+}$ was calculated by density functional theory and periodic boundaries, and its binding energy and stability were discussed. Combined with the first-principles molecular dynamics relaxation behavior and Extended X-ray absorption fine structure (EXAFS) spectral features were used to determine the optimal stable configuration and hydration number, and the bonding mechanism was analyzed by Mulliken charge population, partial wave density of states and differential charge density. The low-energy optimization results show that conformations with hydration numbers 6, 7 and 8 may exist, and there is no obvious boundary between the first and second hydration layers of Pb(II) in the kinetic relaxation process, and the hydration number of the dominant configuration is 6, belonging to the hemidirected configuration. The Pb-O bond in $Pb(H_2O)_6^{2+}$ has strong ionicity, and the bonding mechanism is mainly the coupling between the Pb6p6d orbital and the Pb6s-O2p anti-bonding state orbital, and there is electron filling in the anti-bonding state, which is manifested as a decrease in the electron density between atoms.

Key words Pb(II); hydrated structure; density functional theory; first-principles molecular dynamics; density of states

1. Introduction

As a common heavy metal pollutant, lead exists widely in water, atmosphere, soil and other environments, threatening human health and ecological environment security [1-3]. The current research work mainly focuses on the removal of lead, including chemical precipitation, ion exchange, electrolysis, adsorption, etc. [4-6]. The relevant reaction processes all need to be carried out in an aqueous system, and the metal in the system usually exists in the divalent oxidation state (electron configuration $[Xe]4f^{14}5d^{10}6s^26p^0$). Its complexes exist in two configurations: Holo-directed and Hemi-directed (Fig. 1)[8,9], and the low-coordination (2-5) is a hemi-directed configuration. When the coordination number is high (9-10), it is a holodirected configuration, and both configurations can exist between the coordination numbers 6-8.

Basic research on the structure and related properties of Pb(II) in aqueous solution will help to provide a theoretical reference for the related chemical or biological reactions of this ion in solution whose type is unclear.

In terms of experiments, Swift et al. [10] first determined the average hydration number of the first layer of Pb(II) by NMR to be 5.7, but it was questioned [11,12], because under the same technical

[1] * E-mail: juaner80@163.com; shuweixia@ouc.edu.cn
Received April 4, 2013; published April 10, 2013.
Project supported by the National Natural Science Foundation of China (No. 20677053).

English Translation by Cory Pye. This translation is provided as-is for ease of understanding by English readers. Permission granted by Dr. Xia Yang, Managing Editor of *Acta Chimica Sinica*, Feb 7, 2022.

conditions, the average hydration numbers of Mg(II) and Ca(II) are 3.8 and 4.3, respectively, which are inconsistent with the corresponding hydration numbers of 6 and 6-10 obtained from recent theoretical calculations and experimental data, respectively. In 2011, Persson et al. [13] obtained an average Pb-O bond length of 2.54 Å in the vicinity through EXAFS (extended X-ray absorption fine structure) and LAXS (large-angle X-ray scattering), and the most likely hydration number is 6 (hemidirected configuration), but this technique has certain limitations, only the average bond length of the Pb—O bond can be measured, and the microstructure of Pb(II) in aqueous solution cannot be given.

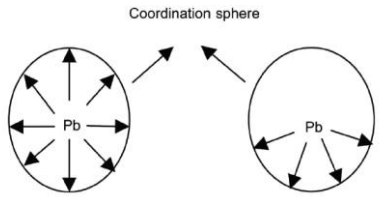


Fig.1 Holodirected configuration (left) and hemidirected configuration (right) of Pb(II) complexes

In terms of theoretical calculation, ab initio calculation and dynamic simulation give different results respectively: Hofer et al. [12,14] used the ab initio QM/MM (quantum mechanical/molecular mechanical) molecular dynamics method based on HF (Hartree-Fock) method. It is found that the hydration number of Pb(II) is 9, and it has an holodirected configuration. The HF method here does not involve electron correlation, and its accuracy is lower than that of the density functional method. Gourlaouen et al. [15] used ab initio and first-principles molecular dynamics simulations to obtain that Pb(II) has a hydration number of 7 and an holodirected configuration. The method did not mention whether the water molecules around lead were randomly distributed according to the solution density before the simulation, which is very important under the limited simulation time of first-principles molecular dynamics. Wander et al. [16] used Gaussian03/DFT to calculate the thermodynamic properties and used the polarized continuum model (PCM) to discuss the solvent effect, and obtained that the coordination number of Pb(II) and H_2O molecules can be 6-8, in which the holodirectional configuration is used. The coordination number 8 is dominant. The recent QMCF (quantum mechanical charge field) method [17] corrected the hydration number of Pb(II) to be 7-9 (mainly 8 coordination, holodirected), this method did not consider the influence of non-Coulomb interaction between solute and solvent, and the handling of particle charges is limited by the radius of action. It can be seen that the solvation structure of Pb(II) in aqueous solution is quite different from the experimental and theoretical calculations, and needs to be further explored.

Statistical calculation of metal ion hydration number by radial distribution function using classical dynamic force field method has been reported [18,19]. However, many force fields (compass, pcff, cvff, etc.) lack the parameter setting for Pb(II), and for the universal force field that involves the most extensive elements at present, it loses "fineness" while seeking "completeness" [20]. Therefore, first-principles molecular dynamics has become one of the indispensable options.

In this paper, the first-principles based on density functional theory are used to study the equilibrium geometry, corresponding binding energy and stability of $Pb(H_2O)_{1\text{-}9}^{2+}$ under periodic conditions. First-principles molecular dynamics was used to explore the relaxation evolution behavior of Pb(II) in aqueous solution, determine its optimal stable configuration and hydration number, and

English Translation by Cory Pye. This translation is provided as-is for ease of understanding by English readers. Permission granted by Dr. Xia Yang, Managing Editor of *Acta Chimica Sinica*, Feb 7, 2022.

analyze its bonding by Mulliken charge distribution, partial wave density of states and differential charge density mechanism and properties.

2 Results and discussion

2.1 $Pb(H_2O)_{1-9}^{2+}$ geometry

The low-energy geometric configuration of $Pb(H_2O)_{1-9}^{2+}$ is calculated from the GGA (generalized gradient approximation) PBE (Perdew-Burke-Ernzerhof) exchange correlation functional, as shown in Figure 2. It can be seen that with the increase of the number of coordinated water molecules, the geometric configuration of species gradually changes from hemidirected ($n \leqslant 5$) to holodirected. For the species configuration where n is 6, it can be regarded as a transition state from hemidirected configuration to holodirected configuration, but closer to the hemidirected configuration. The omnidirectional tendency of hydrated species with n>6 is becoming more and more obvious, but the orientation of the lone pair electrons still occupies a large space. The configuration transition of Pb(II) hydrated species is mainly related to the lone pair of electrons in the 6s orbital, which is called "stereochemically active electron pair", and its existence makes the charge distribution of lead ions nonspherical, resulting in the significant inhomogeneity of ligand distribution around the ion.

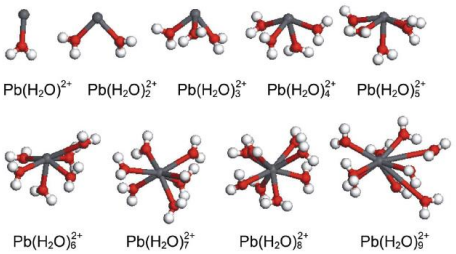


Fig.2 Equilibrium geometry of $Pb(H_2O)_{1-9}^{2+}$ under the periodic condition of GGA-PBE functional

The bond angle $\angle$OPbO in $Pb(H_2O)_{1-3}^{2+}$ is between 82^{o} and 89^{o}, indicating that there is no hybridization between the 6s of Pb(II) and other orbitals in the same layer, and it is repelled by lone pair electrons. The bond angles are all slightly less than 90^{o}. In addition, for the species with n=9, the optimization process found that there are two water molecules detached from the first hydration layer (R_{Pb-O} > 4 Å), while for the species with n = 1 - 8, the Pb-O bond lengths are all within a reasonable range (R_{Pb-O} < 3.7 Å)[15,17]. From this, it is concluded that the highest possible hydration number of Pb(II) is 8, and the hydration species with n = 9 will not be discussed further.

2.2 $Pb(H_2O)_{1-8}^{2+}$ bond length

The Pb-O bond length of Pb(II) hydrated species is related to its geometric configuration. Table 1 lists the minimum bond length R_{min}, maximum bond length R_{max}, and average bond length R_{mean}, of the 8 hydrated species $Pb(H_2O)_{1-8}^{2+}$, respectively. When Pb(II) is low-coordinated with hydration numbers of 2, 3, the Pb-O bond lengths are equal; when n = 4, 5, the bond length distribution is different; when n = 6, 7 and 8 , the bond length changes greatly, among which n = 6 is the most obvious, R_{min} = 2.44, R_{max} = 3.17, R_{mean} = 2.65. This is consistent with the research results of Gourlaouen et al. [15], who roughly divided the Pb-O bond lengths into three types: < 2.6, 2.6-3.0 and > 3.0 Å. In addition, when the

English Translation by Cory Pye. This translation is provided as-is for ease of understanding by English readers. Permission granted by Dr. Xia Yang, Managing Editor of *Acta Chimica Sinica*, Feb 7, 2022.

hydration number is lower than 6, as the number of water molecules increases, the average bond length of the hydrated species increases in a range of 0.04–0.07 Å; from n = 6, the configuration changes, and the average bond length increases significantly (0.12 Å). The optimization results in Table 1 are generally close to the Gaussian03 software DFT/B3LYP and BLYP methods [16], and slightly lower than the QMCF method [17]. The average Pb-O bond length is lower than that of the 6-coordination, but the experimental value only represents the average distance between Pb(II) and several neighboring O atoms.

Table 1. Equilibrium geometry parameters and binding energy of $Pb(H_2O)_n^{2+}$

n	R_{min}/Å	R_{max}/Å	R_{mean}/Å	$E_{binding}$/ (kcal•mol^{-1})	$E_{neighboring}$/ (kcal •mol^{-1})	Pb charge/e	structure
1			2.31	-62.26		1.78	hemi
2	2.36	2.36	2.36	-112.30	-50.04	1.62	hemi
3	2.40	2.40	2.40	-153.35	-41.05	1.51	hemi
4	2.40	2.54	2.47	-182.64	-29.29	1.46	hemi
5	2.41	2.64	2.53	-208.69	-26.05	1.44	hemi
6	2.44	3.17	2.65	-229.45	-20.76	1.42	hemi/holo
7	2.53	2.81	2.67	-249.28	-19.83	1.43	holo
8	2.51	3.04	2.73	-265.65	-16.37	1.44	holo

2.3 $Pb(H_2O)_{1\text{-}8}^{2+}$ binding energy

The binding energy of Pb(II) with H_2O in aqueous solution (Table 1) can be calculated from equation (1):

$$E_{\text{binding}} = E_{\text{Pb}(\text{H}_2\text{O})_n^{2+}} - E_{\text{Pb}^{2+}} - nE_{\text{H}_2\text{O}}$$

The binding energies of the reactions are all negative, indicating that the hydration process is exothermic. The more water molecules, the higher the binding energy and the more stable the hydrated species.

$Pb^{2+}(g) + nH_2O(g) \rightarrow Pb(H_2O)_n^{2+}(g)$ (1)

$Pb(H_2O)_n^{2+}(g) + H_2O(g) \rightarrow Pb(H_2O)_{n+1}^{2+}(g)$ (2)

In order to examine the difficulty of transformation of adjacent hydrated species, the adjacent binding energies between species were calculated from reaction equation (2) (Table 1).

$$E_{\text{neighboring}} = E_{\text{Pb}(\text{H}_2\text{O})_{n+1}^{2+}} - E_{\text{Pb}(\text{H}_2\text{O})_n^{2+}} - E_{\text{H}_2\text{O}}$$

The adjacent binding energies decrease with the increase of the hydration number, gradually approaching the formation of stable species. When n is 6 and 7, the adjacent binding energies are not much different, and when n is 8, it is slightly smaller, indicating that the three reactions are equally difficult.

2.4 Mulliken charge of Pb(II)

Based on the optimized configuration of $Pb(H_2O)_{1\text{-}8}^{2+}$, the Mulliken charge of Pb atom was calculated [21] (Table 1), For n = 1 - 5, the charge of Pb atom gradually decreased from +1.78 to +1. 44, indicating

English Translation by Cory Pye. This translation is provided as-is for ease of understanding by English readers. Permission granted by Dr. Xia Yang, Managing Editor of *Acta Chimica Sinica*, Feb 7, 2022.

that the increase in the number of water molecules reduces the ionicity of Pb. For n⩾6, with the increase of water molecules, the configuration of hydrated species changes, the Pb-O bond distance increases, and the interaction between Pb and O weakens. Finally,the charge of the Pb atom in the final three hydrated species is similar to that of n = 5, and does not show a downward trend.

To sum up, regardless of the average Pb-O bond length, the adjacent binding energy of the hydrated species, or the Mulliken charge of the Pb atom, the species with hydration numbers of 6, 7 and 8 are relatively close, which is consistent with the results of the literature [16]. The hydration free energy of $Pb(H_2O)_{6\text{-}8}^{2+}$ is within 10 kcal/mol of the experimental value calculated by DFT calculation of Gaussian03 software. Controversy about $Pb(H_2O)_5^{2+}$ is also mainly focused on these three hydrates. To this end, the first-principles molecular dynamics method was used to select $Pb(H_2O)_5^{2+}$ as the research object to observe its relaxation behavior in aqueous solution.

2.5 Molecular dynamics simulation

The conformation of $Pb(H_2O)_5^{2+}$ in an aqueous solution with a density of 1.0×10^3 kg/m^3 under periodic boundary conditions is shown in Figure 3. During the kinetic relaxation process, the Pb(II) hydrated species always exist in a partial hemidirected configuration. The dynamic relaxation trajectories of the molecules were statistically analyzed, and the average hydration number of Pb(II) in aqueous solution was calculated based on the radial distribution function.

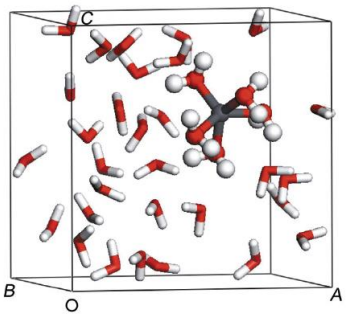


Fig. 3 $Pb(H_2O)_5^{2+}$ localization in an aqueous solution with a density of 1.0×10^3 kg/m^3 under periodic conditions

2.5.1 Radial distribution function

The radial distribution function $g_{ij}(r)$ represents the probability of another atom appearing at a distance r from a central atom. The radial distribution functions of O and H atoms in Pb(II) and water molecules are shown in Fig. 4, both of which show a good first hydration layer definition. The maximum value of the first peak of $g_{Pb\text{-}O}(r)$ appears at 2.57 Å, which represents the average bond length of Pb-O in the first hydration layer. Between r = 3.2 - 3.8 Å, $g_{Pb\text{-}O}(r)$ does not change much, indicating that there is no obvious boundary the first and second hydration layers of Pb(II), and there is an water molecule exchange between the hydrated layers. The maximum value of the first peak of $g_{Pb\text{-}H}(r)$ appears at 3.17 Å, which is consistent with the maximum value of the Pb-H radial distribution function obtained by Gaussian03 first-principles molecular dynamics simulation at 3.2 Å[15].

2.5.2 Ionic hydration number

The coordination number $n_{ij}(r)$ around the metal ion can be calculated by the following formula:

English Translation by Cory Pye. This translation is provided as-is for ease of understanding by English readers. Permission granted by Dr. Xia Yang, Managing Editor of *Acta Chimica Sinica*, Feb 7, 2022.

$$n_{ij}(r) = 4\pi\rho_j \int_0^r r^2 g_{ij}(r) dr \,, \quad (3)$$

where ρ_j is the number density and $g_{ij}(r)$ is the radial distribution function. Figure 4 shows the continuous integration quantile curves of Pb-O and Pb-H atom pairs. Integrating the first peak of $g_{Pb\text{-}O}(r)$, taking r = 2-3.7 Å [15], we get that the average first hydration number of Pb(II) is 6.3, that is, in the first hydration layer, Pb(II) is mainly coordinated by $6H_2O$, which is consistent with the experimental results [10,13]. Therefore, the properties of $Pb(H_2O)_6^{2+}$ are further analyzed below to understand the electron arrangement and bonding mechanism of Pb(II) combined with water molecules in aqueous solution.

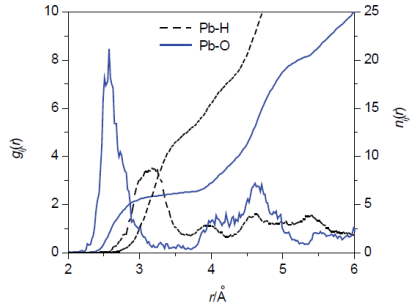


Fig.4. Radial distribution functions of Pb-O and Pb-H and corresponding continuous integral distribution

2.6 $Pb(H_2O)_6^{2+}$ chemical properties

2.6.1 Mulliken population analysis

The electron occupancy number and atomic net charge of each atomic orbital of Pb and O in $Pb(H_2O)_6^{2+}$ are shown in Table 2. Because the gain and loss of electrons of Pb and O atoms are mainly investigated, the orbital population of H atom is not listed. It can be seen from Table 2 that Pb loses some valence electrons and has a charge of +1.42, O gains electrons and has a charge of about -1.00, and the six O atoms have slightly different charges due to different binding positions with Pb. From the number of orbital electrons occupancy, it can be seen that the main orbitals for the formation of $Pb(H_2O)_6^{2+}$ are O2p and Pb6p. Since the supersoft pseudopotential only reflects the interaction between the ion and valence electrons, the Pb6d orbital is not involved here, but theoretical analysis shows that for Pb(II) to combine with 6 H_2O, the Pb6d orbital contribution is indispensable.

Table 2. Charge population of Pb and O atoms

Element	Numbers	s	p	d	f	total charge	charge
O	1	1.86	5.12	0.00	0.00	6.98	-0.98
O	2	1.87	5.14	0.00	0.00	7.01	-1.01
O	3	1.86	5.12	0.00	0.00	6.98	-0.98
O	4	1.86	5.15	0.00	0.00	7.01	-1.01
O	5	1.87	5.14	0.00	0.00	7.00	-1.00
O	6	1.87	5.15	0.00	0.00	7.02	-1.02
Pb	1	1.90	0.68	10.0	0.00	12.58	1.42

English Translation by Cory Pye. This translation is provided as-is for ease of understanding by English readers. Permission granted by Dr. Xia Yang, Managing Editor of *Acta Chimica Sinica*, Feb 7, 2022.

Table 3 lists the bonding populations of Pb and O in $Pb(H_2O)_6^{2+}$. The overlapping population numbers indicate that the Pb-O bond is highly ionic and weakly covalent. However, the overall electronic charge overlap of Pb and O is small, corresponding to weaker bonds and longer bond lengths (up to 3.17 Å). The population numbers of Pb and the first five Os are all negative, indicating that electrons are filled in antibonding orbitals, which is not uncommon for heavy metals containing "stereochemically active electron pairs". The asymmetric structure has also been reported to be related to the filling of antibonding states [22,23], which is not due to the hybridization of the metal ns-np orbital making the electron pair stereoactive, but because the electron filling is in the metal ns that are closer in energy level to the ligand. On the antibonding orbital formed by the bulk np, the high energy level of the antibonding state is not conducive to the stability of the compound, and finally the structure of the compound is deformed.

Table 3. Overlap population analysis of Pb-O bonds

Bond	population number	bond length/Å
Pb-O(1)	-0.04	2.44
Pb-O(2)	-0.02	2.60
Pb-O(3)	-0.05	2.48
Pb-O(4)	-0.04	2.54
Pb-O(5)	-0.02	2.64
Pb-O(6)	0.01	3.17

2.6.2 Density of States

The partial wave density of states (PDOS) of O and Pb in $Pb(H_2O)_6^{2+}$ is shown in Fig. 5. In Fig. 5(a), the peak at -17 – -19 eV mainly corresponds to the O2s orbital. The locality is enhanced, mainly contributed by O2p, supplemented by O2s (here mainly related to the sp^3 hybridization of O in H_2O), and the conduction band part is mainly distributed between 5 and 10 eV. For the PDOS diagram of Pb [Fig. 5(b)] in the middle valence band, Pb5d corresponds to a high peak at -13 – -15 eV, the electron distribution is relatively localized, the number of electrons in this orbital is large, and the energy levels are similar. In addition, the Pb6s state appears at -7 – -5 eV (region I), -4 to 0.5 eV (region II) and 5 to 10 eV (region III), the Pb6p contribution mainly appeared near regions II and III.

The energy level increase of Pb6s state (region II is close to the Fermi level) may be mainly related to the combination of Pb6s and O2p with similar energy in antibonding state; hybridization with antibonding filled orbitals [24], and the existence of partial region III in the conduction band is also one of the proofs.

2.6.3 Differential charge density

The difference in charge density of $Pb(H_2O)_6^{2+}$ relative to Pb is shown in Fig. 6, the isodensity difference is ±0.025 electrons/$Å^3$, the absence of electrons is represented by blue, and the enrichment is represented by red. In both Pb atom (mark 1) and O atom (mark 4) electron enrichment appears, which is characteristic of Pb—O bonding. There are electron reduction regions around Pb (mark 2) and O (mark 3), especially the reduction of electron density around Pb is very obvious, which once again proves the existence of electron filling in the antibonding state between Pb-O. The loss of electrons around the H atom (mark 5) is mainly due to the transfer of electrons to the strongly electronegative O atom.

English Translation by Cory Pye. This translation is provided as-is for ease of understanding by English readers. Permission granted by Dr. Xia Yang, Managing Editor of *Acta Chimica Sinica*, Feb 7, 2022.

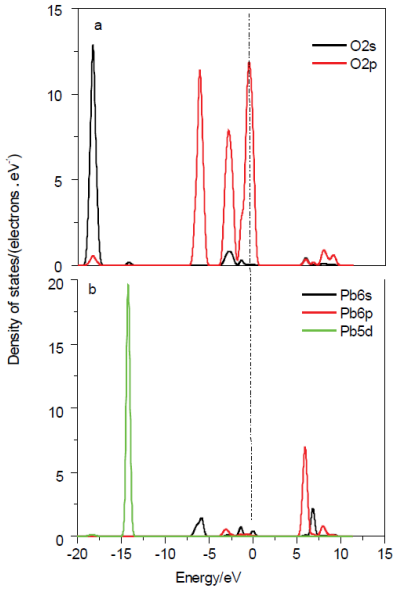


Figure 5. The partial wave density of states of O and Pb in $Pb(H_2O)_6^{2+}$

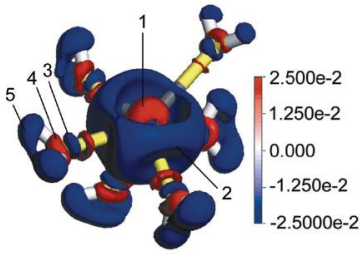


Figure 6. Differential charge density of $Pb(H_2O)_6^{2+}$ relative to Pb

In conclusion, the results of this study support the theory that the antibonding state filling causes the chemical activity of lone pair electrons, mainly based on the following three points:

(1) The bond angle ∠OPbO in $Pb(H_2O)_{1\text{-}3}^{2+}$ ranges from 82° to 89°, which proves that Pb6s is not hybridized with the Pb6p6d orbital, and the incomplete overlap of the density of states of Pb6s and Pb6p in the PDOS diagram of Pb also proves that at this point.

(2) The negative Mulliken population of the Pb-O bond, the increase of the Pb6s energy level in PDOS, and the large reduction of the electron density between atoms after Pb-O bonding all prove the existence of the electron filling of the Pb6s-O2p antibonding state.

(3) In PDOS, the Pb6p and antibonding states (Pb6s-O2p) overlap in region II, which proves that the combination of the antibonding states makes the orbital energy level close to that of Pb6p6d, and then coupling occurs.

3. Conclusions

Using first-principles density functional theory, GGA-PBE exchange-correlation potential, under periodic boundary simulation conditions, the maximum possible hydration number of Pb(II) is 8. The hydrated species $Pb(H_2O)_{1\text{-}8}^{2+}$ has a hydration number of 6 as the transition coordination number of the

hemidirected configuration and the holodirected configuration; the bond length, binding energy and Mulliken charge analysis show that the hydration numbers 6, 7 and 8 all may exist. Combined with the Pb-O radial distribution function of first-principles molecular dynamics, as well as the experimental EXAFS and LAXS results, it is concluded that the hydrated species of Pb(II) in aqueous solution are mainly in the form of $Pb(H_2O)_6^{2+}$ partial hemidirected configuration. The Pb-O bond in $Pb(H_2O)_6^{2+}$ is weak in covalency and strong in ionicity.The bonding mechanism is mainly the coupling between Pb6p6d and Pb6s-O2p antibonding orbitals.

4. Experimental

Quantum chemical calculations are all completed by the relevant modules of the Material studio software package [25].

The ionic hydration species were constructed by Visualizer module, the geometric configuration optimization and corresponding property analysis were completed by Castep module [26], using density functional theory [27,28], GGA-PBE [29] exchange correlation potential, supersoft pseudopotential[26] 30], BFGS (Broyden-Fletcher-Goldfarb-Shanno) geometric optimization method [31], using delocalized coordinates, reciprocal space, 340 eV cut-off energy, convergence criteria: energy difference is 1.0×10^{-5} eV/atom, energy The gradient is 0.03 eV/Å. The Brillouin zone integration uses the Monkhorst-Pack method to generate k-point sampling grids in 3 lattice directions [32], using a period box of 10 Å×10 Å×10 Å for the studied system 1×1×1 grid, the Fermi energy is calculated using the Gaussian band broadening method.

The kinetic simulation uses the construction function of the Amorphous cell module to put $Pb(H_2O)_5^{2+}$ into a periodic box containing 30 water molecules, the density of water molecules is 1.0×10^3 kg/m^3, and the universal force field of the Forcite module is used[33,34] The system was geometrically optimized to make it randomly distributed, the H_2O molecule was the TIP3P model [35], the atomic charges in $Pb(H_2O)_5^{2+}$ were obtained by the QEq method [36], and the van der Waals and electrostatic interactions were obtained by the Atom-based method [35]. 37] and Ewald sum method [38], the non-bonding cutoff radius is 5.5 Å. Castep module GGA-PBE exchange correlation potential, supersoft pseudopotential, 300 eV cutoff energy, 1×1×1 grid k-point sampling, select Molecular dynamics simulations were run on the NVT ensemble, T = 298 K, temperature control using Nose algorithm [39], step size 1.0 fs, simulation 8.0 ps, and all atomic coordinates were allowed to freely change during the simulation.

References

[1] Markus, J.; McBratney, A. B. *Environ*. *Int*. **2001**, *27*, 399.

[2] Loef, M.; Mendoza, L. F.; Walach, H. *Toxin Rev*. **2011**, *30*(4), 103.

[3] Olympio, K. P. K.; Goncalves, C.; Günther, W. M. R.; Bechara, E. J. H. *Rev*. *Panam*. *Salud Publica/Pan*. *Am*. *J*. *Public Health* **2009**,*26*(3), 266.

[4] Unuabonah, E. I.; Olu-Owolabi, B. I.; Oladoja, A. N.; Ofomaja, A. E.; Yang, Z. L. *J*. *Soil*. *Sediment*. **2010**, *10*, 1103.

[5] Zhang, D.; Hou, P. *Acta Chim*. *Sinica* **2009**, *67*(12), 1336.

English Translation by Cory Pye. This translation is provided as-is for ease of understanding by English readers. Permission granted by Dr. Xia Yang, Managing Editor of *Acta Chimica Sinica*, Feb 7, 2022.

[6] Jiang, M. Q.; Wang, Q. P.; Jin, X. Y.; Chen, Z. L. *J*. *Hazard*. *Mater*. **2009**, *170*, 332.

[7] Parr, J. *Polyhedron* **1997**, *16*(4), 551.

[8] Shimoni-Livny, L.; Glusker, J. P.; Bock, C. W. *Inorg*. *Chem*. **1998**, *37*, 1853.

[9] Gourlaouen, C.; Gerard, H.; Piquemal, J.-P.; Parisel, O. *Chem*. *Eur*. *J*. **2008**, *14*, 2730.

[10] Swift, T. J.; Sayre, W. G. *J*. *Chem*. *Phys*. **1966**, *44*(9), 3567.

[11] Marcus, Y. *J*. *Chem*. *Soc*. *Faraday Trans*. **1991**, *87*, 2995.

[12] Hofer, T. S.; Rode, B. M. *J*. *Chem*. *Phys*. **2004**, *121*, 6406.

[13] Persson, I.; Lyczko, K.; Lundberg, D.; Eriksson, L.; Placzek, A. *Inorg*. *Chem*. **2011**, *50*, 1058.

[14] Hofer, T. S.; Randolf, B. R.; Rode, B. M. *Chem*. *Phys*. **2006**, *323*, 473.

[15] Gourlaouen, C.; Gerard, H.; Parisel, O. *Chem*. *Eur*. *J*. **2006**, *12*, 5024.

[16] Wander, M. C. F.; Clark, A. E. *Inorg*. *Chem*. **2008**, *47*, 8233.

[17] Bhattacharjee, A.; Hofer, T. S.; Pribil, A. B.; Randolf, B. R.; Lim, L. H. V.; Lichtenberger, A. F.; Rode, B. M. *J*. *Phys*. *Chem*. *B* **2009**, *113*, 13007.

[18] Li, F. *M.S. Thesis*. Hebei University of Technology, Tianjin, **2011**.

[19] Sun, W.; Chen, Z.; Huang, S. Y. *J*. *Wuhan Univ*. *Tech*. **2005**, *27*(7), 26.

[20] Ji, Q.; Yang, X. Z. *Chemistry Online* **2005**, *2*, 111.

[21] Mulliken, R. S. *J*. *Chem*. *Phys*. **1955**, *23*, 1833.

[22] Mudring, A. V.; Rieger, F. *Inorg*. *Chem*. **2005**, *44*, 6240.

[23] Mudring, A. V. *Eur*. *J*. *Inorg*. *Chem*. **2007**, *2007*(6), 882.

[24] Walsh, A.; Watson, G. W. *J*. *Solid State Chem*. **2005**, *178*, 1422.

[25] *Materials Studio 4. 3*. San Diego, CA, Accelrys Inc., **2008**.

[26] Clark, S. J.; Segall, M. D.; Pickard, C. J.; Hasnip, P. J.; Probert, M. J.; Refson, K. *Z*. *Kristallogr*. **2005**, *220*, 567.

[27] Hohenberg, P.; Kohn, W. *Phys*. *Rev*. **1964**, *136*(3B), B864.

[28] Kohn, W.; Sham, L. J. *Phys*. *Rev*. **1965**, *140*(4A), A1133.

[29] Perdew, J. P.; Burke, K.; Ernzerhof, M. *Phys*. *Rev*. *Lett*. **1996**, *77*, 3865.

[30] Vanderbilt, D. *Phys*. *Rev*. *B* **1990**, *41*(11), 7892.

[31] Pfrommer, B. G.; Cote, M.; Louie, S. G.; Cohen, M. L. *J*. *Comput*. *Phys*. **1997**, *131*, 233.

[32] Monkhorst, H. J.; Pack, J. D. *Phys*. *Rev*. *B* **1976**, *13*(12), 5188.

English Translation by Cory Pye. This translation is provided as-is for ease of understanding by English readers. Permission granted by Dr. Xia Yang, Managing Editor of *Acta Chimica Sinica*, Feb 7, 2022.

[33] Rappe, A. K.; Colwell, K. S.; Casewit, C. J. *Inorg*. *Chem*. **1993**, *32*, 3438.

[34] Casewit, C. J.; Colwell, K. S.; Rappe, A. K. *J*. *Am*. *Chem*. *Soc*. **1992**, *114*, 10046.

[35] Jorgensen, W. L.; Chandrasekhar, J.; Madura, J. D.; Impey, R. W.; Klein, M. L. *J*. *Chem*. *Phys*. **1983**, *79*, 926.

[36] Rappe, A. K.; Goddard, W. A. *J*. *Phys*. *Chem*. **1991**, *95*(8), 3358.

[37] Karasawa, N.; Goddard, W. A. *Macromolecules* **1992**, *25*, 7268.

[38] Ewald, P. P. *Ann*. *Phys*. **1921**, *64*, 253.

[39] Nose, S. *Mol*. *Phys*. **1984**, *52*, 255.